Journal of Applied Polymer Science

Morphology, Interfacial Interaction, and Properties of a Novel Bioelastomer Reinforced by Silica and Carbon Black

Runguo Wang,[1] Hui Yao,[1] Weiwei Lei,[1] Xinxin Zhou,[1] Liqun Zhang,[1,2] Kuo-chih Hua,[3] Joseph Kulig[3]

[1]Key Laboratory of Beijing City for Preparation and Processing of Novel Polymer Materials, Beijing University of Chemical Technology, Beijing 100029, People's Republic of China

[2]State Key Laboratory of Organic-Inorganic Composites, Beijing University of Chemical Technology, Beijing 100029, People's Republic of China

[3]Goodyear Innovation Center, Goodyear Tire & Rubber Company, Akron, Ohio 44309-3531

Correspondence to: L. Zhang (E-mail: zhanglq@mail.buct.edu.cn)

ABSTRACT: A novel poly(diisoamyl itaconate-*co*-isoprene) (PDII) bioelastomer was prepared by redox emulsion polymerization based on itaconic acid, isoamyl alcohol, and isoprene. Carbon black (CB), silica, and silica with coupling agent (*bis*(3-(triethoxysilyl)-propyl)tetrasulfide [TESPT]-silica) were used as fillers to reinforce the novel elastomer. The difference in morphology, interfacial interaction, thermal properties, and mechanical properties of PDII composites filled with different fillers was studied. The homogeneous dispersion of silica and CB in the PDII matrix was confirmed by scanning electron microscopy and transmission electron microscopy. Silica had homogenous dispersion possibly because of the formation of hydrogen bonds between the silica silanols and the PDII macromolecular chains. PDII/silica and PDII/TESTP-silica have lower crosslink density and crosslinking rate than PDII/CB owing to the adsorption of accelerators by the silanols in the silica surfaces. PDII/silica had comparable tensile strength but higher elongation at break than PDII/CB. The tensile strength of PDII/TESPT-silica was higher than PDII/CB and PDII/silica. © 2012 Wiley Periodicals, Inc. J. Appl. Polym. Sci. 129: 1546–1554, 2013

KEYWORDS: biopolymers and renewable polymers; composites; elastomers; nanoparticles

Received 4 July 2012; accepted 19 November 2012; published online 15 December 2012
DOI: 10.1002/app.38865

INTRODUCTION

Because of its unique high elasticity, elastomer, generally acknowledged as a crucial strategic material, finds wide applications in industry, national defense, cutting-edge technology, and our daily life.[1–3] The basic building blocks of synthetic rubber, such as butadiene, styrene, and chloroprene, are currently mainly derived from crude oil. However, the nonrenewable crude oils will last only for 46.2 years according to the BP Statistic Review of World Energy 2011. To tackle this global scientific issue, a new strategy is put forward to prepare polymeric materials from renewable resources such as biomass.[4,5] Some bioelastomers, which have potential use in tissue engineering, drug delivery, and vivo sensing,[6–14] have been recently reported, especially polyester and poly(amide ester) elastomers. However, the monomers in these pioneering studies were not required to be derived from biomass—they just had to be biocompatible, with degradation products which were nontoxic to human bodies. These bioelastomers are not suitable for engineering application owing to lower tensile strength and much higher cost than conventional elastomers. Itaconic acid was a bio-based chemical which could be produced in large scale (above 80,000 ton/year) by fermentation and sold at low price (around $2/kg). In this study, a novel crosslinkable poly(diisoamyl itaconate-*co*-isoprene) (PDII) elastomer with high molecular weight was synthesized by redox emulsion polymerization based on itaconic acid, isoamyl alcohol, and isoprene. Itaconic acid and isoamyl alcohol are produced by fermentation of biomass like corn starch.[15–18] Bioisoprene technology was highly developed by Genencor (Palo Alto, CA) and Amyris (Emeryville, CA), which announced large-scale manufacture by 2012 and 2015, respectively.[19,20] The number average molecular weight of the PDII elastomer was above 300,000 and the glass transition temperature was below −30°C. However, the tensile strength of the neat PDII vulcanizates was only 1.1 MPa, which are not suitable for many engineering applications. Thus, fillers should be used to reinforce the PDII elastomer.

The reinforcement of elastomer by fillers enhances the physical properties, such as hardness, modulus, tensile strength, and abrasion resistance, of the elastomer.[21,22] Among various fillers, carbon black (CB) is the most important reinforcing agent used

in the rubber industry owing to its low cost and significant reinforcement.[23,24] However, CB causes pollution because of its origin from petroleum and gives the rubber a black color (which is undesirable in certain applications). In the last decades, research was focused on the development of other reinforcing agents such as silica,[25] inorganic fibers,[26] organic whiskers,[27] carbon nanotubes,[28] and layered silicate clays[29] to replace CB in rubber compounds. Among these other reinforcing agents, silica is regarded as the most promising filler owing to its small particle size, large surface area, petroleum independence, and large-scale production.[30,31] The presence of hydroxyl groups on the surface of silica results in strong filler–filler interactions and tight aggregates.[32] Its property can cause a poor dispersion of silica in a rubber compound. In general, a silane coupling agent such as *bis*(3-(triethoxysilyl)-propyl)tetrasulfide (TESPT) is used to improve the filler dispersion.[33] Differences of CB and silica-reinforced conventional rubbers have been investigated in the last decades. Choi et al. studied the influence of filler type and content on the properties of styrene–butadiene rubber (SBR) and natural rubber (NR) compounds[34,35]; Vo et al. studied the dielectric properties of styrene–butadiene composites with CB, silica, and nanoclay[36]; Mora-Barrantes et al. studied the filler network, physical, and dynamic properties of SBR reinforced by carbon–silica dual-phase filler.[37] However, these studies mainly focused on traditional SBR and NR but not the elastomers with polar groups (e.g., ester groups). The research of morphology, interfacial interaction, and properties of CB and silica-filled novel elastomers with polar groups was necessary and meaningful.

Different from most commercial engineering rubbers, the PDII prepared in this study contains a lot of ester groups. As numerous silanol groups are expected to exist on the surface of silica, we hypothesized that hydrogen–bond interactions would occur between the PDII macromolecules and the silica and be beneficial to fine dispersion and high performance. The hypothesis was proved by the comparison of morphology, interfacial interaction, and properties of CB-filled PDII (PDII/CB), silica-filled PDII (PDII/silica), and silica with coupling agent-filled PDII (PDII/TESPT-silica). The homogeneous dispersion of silica and CB was confirmed by scanning electron microscopy (SEM) and transmission electron microscopy (TEM). The tensile strength of PDII/silica could be further improved by introducing a coupling agent.

EXPERIMENTAL

Materials

Itaconic acid (purity, 99%) was obtained from Langyatai Coporation (Qingdao, China). Isoamyl alcohol (Natural Product; purity, 97%) was purchased from Sigma Aldrich (Shanghai, China). Isoprene (purity, 95%) was purchased from Alfa Asear (Tianjing, China) and distilled to remove stabilizing agent before use. Ferric ethylenediaminetetraacetic acid salt (Fe-EDTA), oleic acid, sodium hydroxymethanesulfinate (SHS), tert-butyl hydroperoxide (TBH), potassium phosphate tribasic, potassium chloride, and hydroxyl amine were purchased from Sigma Aldrich and used without further purification. Precipitated silica (Tixosil 383) with an average particle of 20–40 nm and specific surface area of 100–150 m^2/g (cetyltrimethylammonium bromide [CTAB]) was purchased from Rhodia Company, France. CB (N234) with an average particle of 17-40 nm and specific surface area of 110–130 m^2/g (CTAB) was purchased from Cabot, USA. TESPT was purchased from Nanjing Shuguang Chemical Group, China. All other chemicals for the rubber compounds were reagent-grade commercial products and were used as received without further purification.

Table I. Recipe for Redox-Initiated Emulsion Polymerization

Ingredients	Amount (g)
Diisoamyl itaconate	Variable
Isoprene	Variable
Deionized water	250
Potassium oleate solution (10%)	25
Potassium phosphate tribasic solution (10%)	2
Potassium chloride (10%)	5
SHS solution (10%)	2
Fe-EDTA solution (10%)	0.4
TBH toluene solution (10%)	0.5
Hydroxyl amine solution (50%)	0.4

Synthesis of PDII

Diisoamyl itaconate was prepared by the esterification of itaconic acid and isomayl alcohol by the previously published methods.[38] The polymerization reactor was a 1-L four-neck glass flask equipped with a reflux condenser, a sampling device, a nitrogen inlet and a two-bladed anchor-type impeller. As summarized in Table I, deionized water, potassium oleate solution, potassium phosphate tribasic solution, and potassium chloride solution were added into the flask under high-speed stirring (450 rpm). Subsequently, diisoamyl itaconate and isoprene were added into the flask, and the stirring speed was reduced to 250 rpm. A stable homogeneous latex was obtained after 30 min of stirring. Later, the Fe-EDTA solution, SHS solution, and TBH solution were injected into the flask. The polymerization was allowed to proceed at 20°C for 12 h to form the target PDII latex, and the hydroxylamine solution was added to terminate the polymerization. The PDII latex was coagulated using an excess of ethanol and dried at 60°C in vacuum until a constant weight was obtained.

Preparation of PDII Composites

The PDII and additives were mixed by a 6-in two-roll mill according to the formulation provided in Table II. The compound was cured in an XLB-D 350×350 hot press (Huzhou East Machinery, China) under a pressure of 15 MPa at 150°C for its optimum cure time.

Analysis and Characterization

Fourier Transform Infrared Spectroscopy. Infrared spectra of samples were recorded on a Bruker Tensor 27 spectrometer using the attenuated total reflection technique. The spectra were obtained at a resolution of 4 cm^{-1} in the range of 4000–600 cm^{-1}.

Applied Polymer SCIENCE

Table II. Formulations for PDII and PDII Composites

	PDII	PDII/CB	PDII/silica	PDII/ TESPT-silica
PDII gum	100	100	100	100
Carbon black	0	50	0	0
Silica	0	0	50	50
TESPT	0	0	0	5
ZnO	5.0	5.0	5.0	5.0
Stearic acid	0.5	0.5	0.5	0.5
MBT	0.7	0.7	0.7	0.7
CBS	1.0	1.0	1.0	1.0
Sulfur	1.0	1.0	1.0	1.0

Abbreviations: MBT, 2-mercaptobenzothiazole; CBS, *N*-cycolhexyl-2-benzothiazole; TESPT, *bis*(3-(triethoxysilyl)-propyl)tetrasulfide.

^{1}H-NMR Spectroscopy. ^{1}H-NMR spectroscopy was carried out with a Bruker AV400 spectrometer. $CDCl_3$ was used as the solvent for the NMR measurements.

Gel Permeation Chromatography. The molecular weights of PDII, SBR, nature rubber, and acrylic rubber were determined by gel permeation chromatography (GPC) measurements on a Waters Breeze instrument equipped with three water columns (StyragelHT3_HT5_HT6E) using tetrahydrofuran as the eluent (1 mL/min) and a Waters 2410 refractive index detector. A polystyrene standard was used for calibration.

Differential Scanning Calorimetery. Differential scanning calorimetery (DSC) thermograms of neat PDII, PDII/CB, PDII/silica, and PDII/TESPT-silica were recorded in the range from −80 to 200°C on a Mettler-Toledo DSC using a heat rate of 10°C/min under nitrogen.

Dynamic Mechanical Thermal Analysis. The dynamic mechanical properties of neat PDII, PDII/CB, PDII/silica, and PDII/TESPT-silica were measured by using a 01 dB-Metravib VA3000 dynamic mechanical analyzer, France. The test specimens for DMTA were cut from molded PDII sheets, approximately 2.0 mm thick. The runs were made in the tension mode at a fixed frequency of 10 Hz, and a strain amplitude of 0.1%. The temperature range was from −80 to 120°C, and the heating rate was 3°C/min.

Scanning Electron Microscopy. The surface morphology of PDII/CB, PDII/silica, and PDII/TESPT-silica was observed in Hitachi S-4800 scanning electron microscope. The samples were prepared by fracturing the composites in liquid nitrogen and were previously sputter coated with gold.

Transmission Electron Microscopy. An H-800 TEM made by Hitachi in Japan was employed to examine the morphology and distribution of nanoparticles in PDII/CB, PDII/silica, and PDII/TESPT-silica. The TEM specimens of the silica-filled PDII nanocomposites were prepared by cryogenic microtoming using a Reichert-Jung Ultracut Microtome and mounted on 200 mesh copper grids.

Curing Characteristics. The curing characteristics of neat PDII and PDII composites were measured at 150°C with an oscillating disc-rheometer, P3555B2, manufactured by Beijing University of Chemical Technology, China.

Tensile Tests. The tensile tests were conducted according to ASTM D412. All the specimens were dumbbell-shaped in 25-mm gauge length, 6 mm width, and 2 mm thickness. The specimens were tested on a LRX Plus Tensile Tester made by Lloyd Instruments, in United Kingdom.

RESULTS AND DISCUSSION

Characterization of PDII Gums

PDII gum was obtained by the emulsion polymerization of diisoamyl itaconate and isoprene. Schemes 1 and 2 show the preparation method of PDII gums. As summarized in Table III, the number average molecular weight (M_n) is above 350,000, and the polydispersity index is 3.41. By the comparison with conventional rubbers, the PDII gum has similar polydispersity index and comparable M_n with SBR and acrylate rubber. According to the previous polyisoprene-related studies,[39,40] the chemical shift for the $=CH_2$ of 1,2 units is 4.60–4.80 ppm and the chemical shift for $=CH_2$ of 3,4 units was 4.80–5.05 ppm. The chemical shift for the =CH— of *trans*-1,4 units and *cis*-1,4 units was 5.08–5.40 ppm. Figure 1 shows that the chemical shifts for 1,2 units and 3,4 units were absent. Thus, the isoprene units were mostly *trans*-1,4 units and *cis*-1,4 units.

Fourier Transform Infrared Analysis of Neat PDII and PDII Composites

The peaks at 2871, 2921, and 2957 cm^{-1} are attributed to the stretching vibration of C—H groups in PDII (Figure 2). The peaks at 1167 and 1727 cm^{-1} are attributed to the stretching vibration of C—O—C and C=O groups, respectively. No obvious difference was observed between the PDII/CB and the PDII. Peaks can been seen at 1093 and 1099 cm^{-1} for the stretching vibration of the Si—O groups of PDII/silica and PDII/TESPT-silica. The stretching vibrations of C—O—C at 1167 cm^{-1} shift to 1158 and 1164 cm^{-1} for PDII/silica and PDII/TESPT-silica, respectively. As the absorption peak of C—O—C groups shifts from 1167 cm^{-1} for neat PDII to 1158

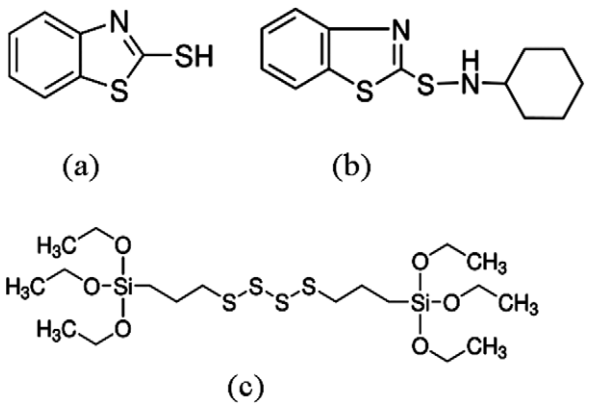

Scheme 1. Chemical structures of (a) MBT, (b) CBS, and (c) TESPT.

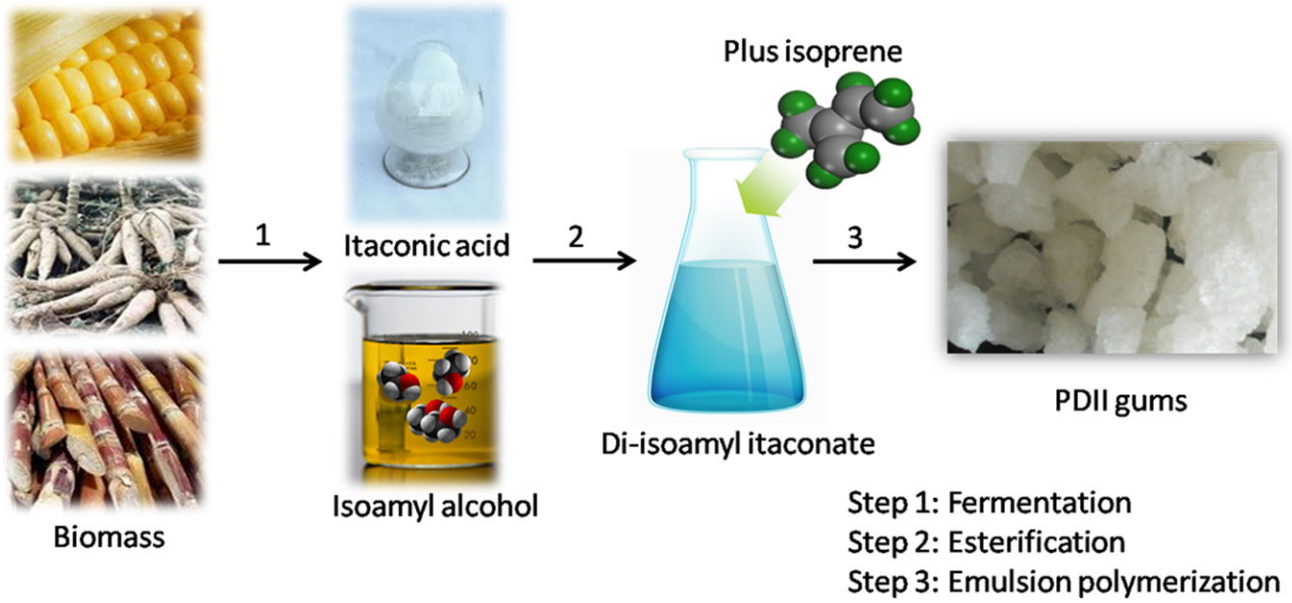

Scheme 2. The preparation strategy of PDII gums. [Color figure can be viewed in the online issue, which is available at wileyonlinelibrary.com.]

cm^{-1} for PDII/silica, we assume that hydrogen bonds were formed between silica silanols and PDII macromolecules as shown in Scheme 3.

Fourier Transform Infrared (FTIR) spectra of PDII/silica composites with different silica contents were carried out to investigate the hydrogen bonds between silica and PDII. Figure 3 shows significant differences in the peaks between 1000 and 1500 cm^{-1} in FTIR spectra. The absorption peak located at 1167 cm^{-1} which attributed to C—O—C stretching vibrations in PDII demonstrates obvious shift with the increase of silica contents, so did the peak located at 1082 cm^{-1} which attributed to Si—O—Si stretching vibration. The facts indicate that the silanol groups formed hydrogen bonds with PDII macromolecular chains.

Morphology of PDII/CB, PDII/Silica, and PDII/TESPT-Silica

To investigate the morphology of CB and silica in the PDII composites, representative fracture surfaces were studied by TEM and SEM. In Figure 4(a–c), the light part represents the PDII matrix and the dark part represents the filler particles that have been densely distributed in the matrix. Figure 4(a–c) shows that silica has comparable homogenous dispersion in the PDII with CB in the PDII. The SEM photographs in Figure 4 (d–f) show that the silica particles having size ranging from 20 to 40 nm in size and are spherical in shape. The silica particles are dispersed in the PDII matrix homogeneously with smaller particle size and fewer agglomerates than conventional silica-filled rubbers, possibly because of the stronger interfacial interaction between the silica and the PDII matrix. Furthermore, the dispersion of silica in the PDII matrix with TESPT is slightly better than the dispersion of silica in the PDII matrix without TESPT. The silane coupling agent has a sulfidic linkage between triethoxysilylpropyl groups. The ethoxy group of the coupling agent reacts with the silanol group of the silica to form a siloxane bond. The bound silane on the silica surface can weaken the filler–filler interaction of silica and prevent the silica from agglomerating.

Table III. Molecular Weights of PDII Gum and Conventional Rubbers

Rubber	$M_n/10^4$ (g/mol)	Polydispersity Index
PDII	35.1	3.41
SBR (1502)	16.5	3.67
NR	39.2	2.47
Acrylic Rubber (K3030)	32.4	3.57

Cure Curves and Mechanical Properties of Neat PDII and PDII Composites

As vulcanization is a vital step for rubber products, we investigated the effect of fillers on curing characteristics. As the

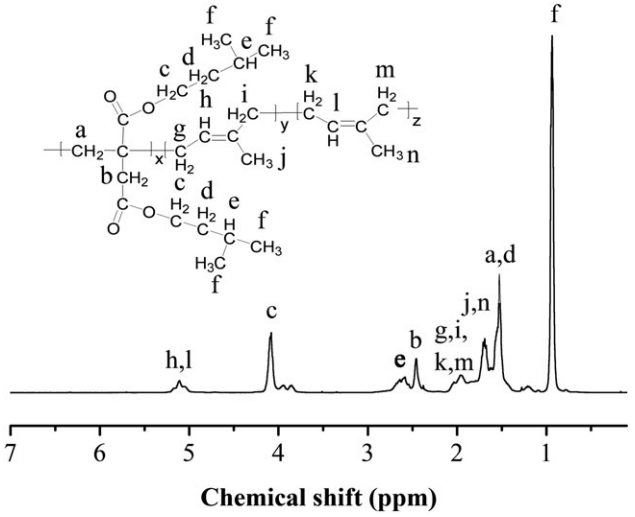

Figure 1. ^{1}H NMR spectrum of PDII with diisomayl itaconate/isoprene mass ratio as 80:20.

Applied Polymer SCIENCE

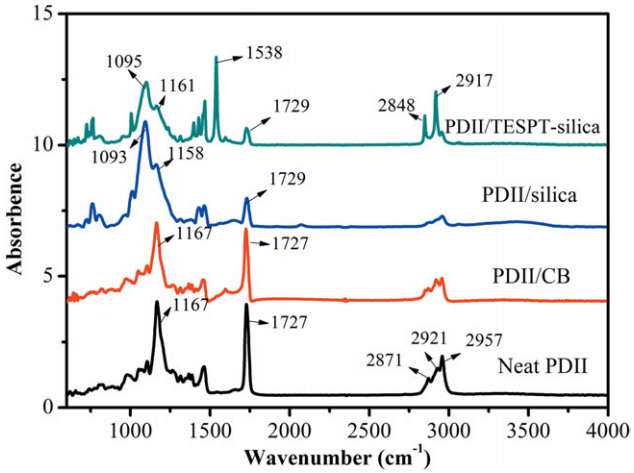

Figure 2. FTIR spectra of PDII and PDII composites. [Color figure can be viewed in the online issue, which is available at wileyonlinelibrary.com.]

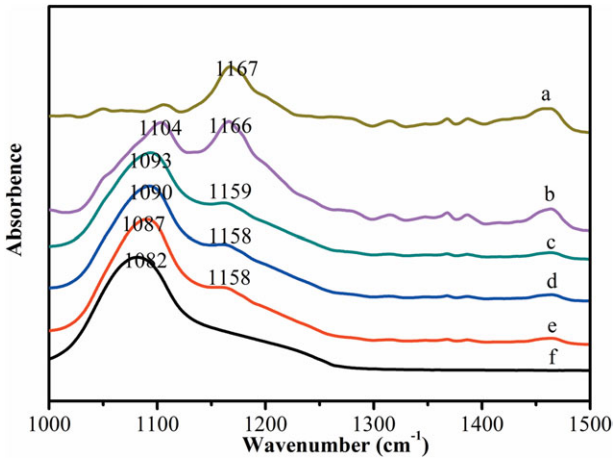

Figure 3. Dependence of FTIR spectra on silica content of the PDII/silica composites, the weight ratio of PDII/silica is (a) 100:0, (b) 80:20, (c) 60:40, (d) 40:60, (e) 20:80, and (f) 0:100. [Color figure can be viewed in the online issue, which is available at wileyonlinelibrary.com.]

modulus of rubber increases dramatically during curing, it is used as a monitor to investigate the progress of curing. Figure 5 and Table IV show the torques in the cure curves of these vulcanizates increase successively with time as s a result of the increase in crosslink density. Shapes of the cure curves of PDII/silica and PDII/TESPT-silica are very different compared with the PDII/CB as shown in Figure 5. The slower curing of the silica-filled compounds than that of PDII/CB can be explained by adsorption of 2-mercaptobenzothiazole (MBT) and *N*-cycolhexyl-2-benzothiazole (CBS) on the silica surface. As silica has many hydroxyl groups, polar materials, especially basic organics, are easily adsorbed on the silica surface. Thus, MBT and CBS molecules can be adsorbed well on the silica surface. The increased adsorption of accelerators makes the cure time and cure rate decrease with filling of silica. The reason for lower cure rate and torque of PDII/TESPT-silica than PDII/silica was

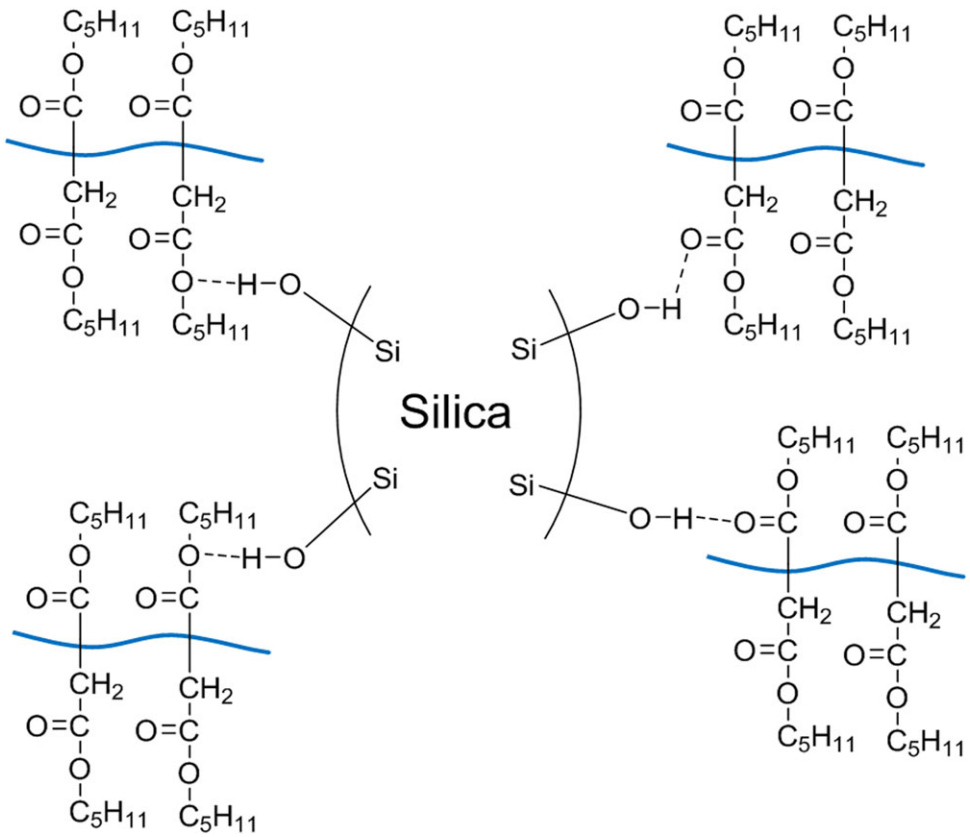

Scheme 3. Possible hydrogen bonds between silica and PDII macromolecules.

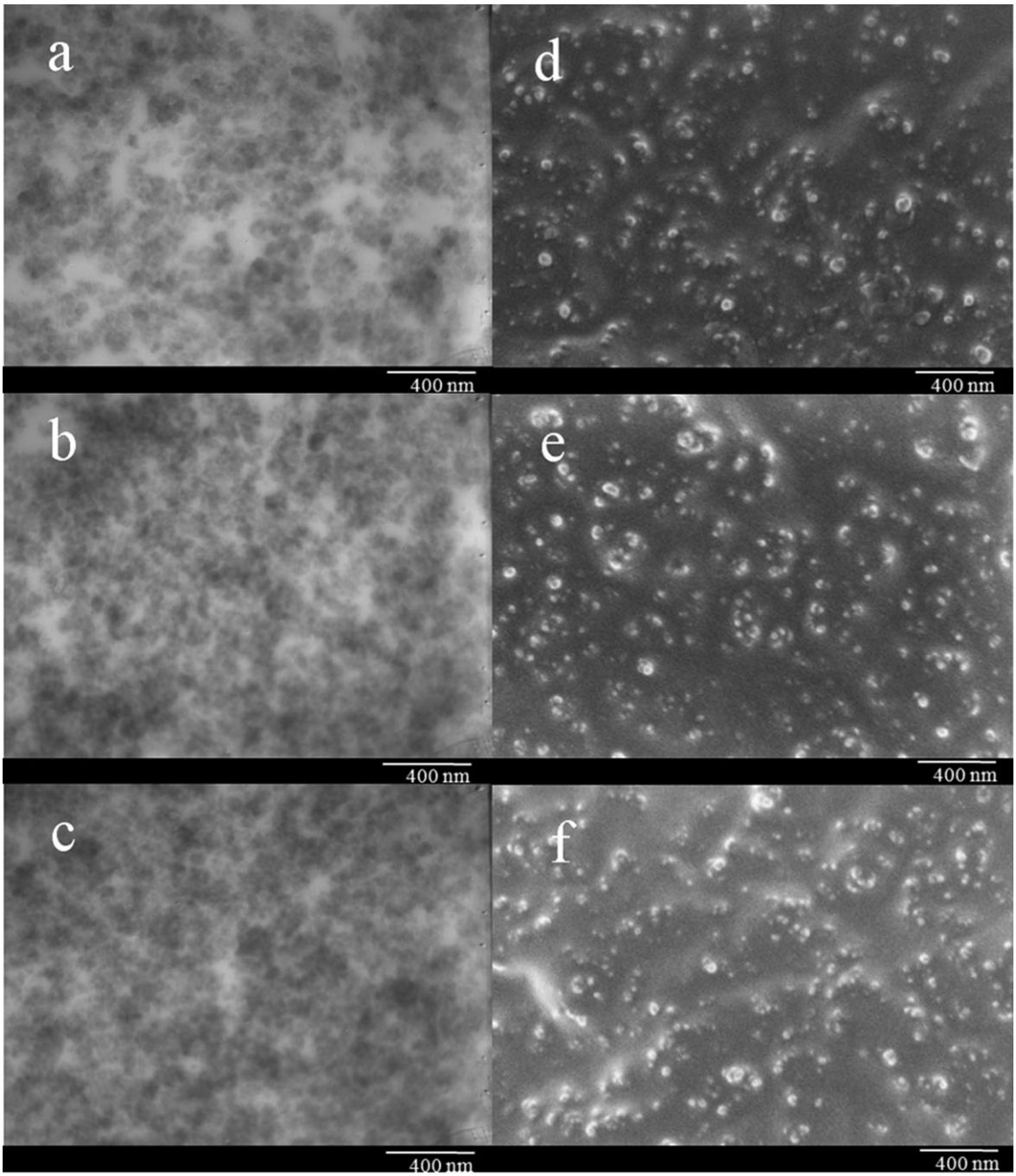

Figure 4. (a–c) TEM observations of PDII composites: (a) PDII/CB, (b) PDII/silica, (c) PDII/TESPT-silica; (d–f) SEM observations of PDII composites: (d) PDII/CB, (e) PDII/silica, and (f)PDII/TESPT-silica.

owing to the use of coupling agent. TESPT was a low-molecular-weight liquid, it acted as a plasticizer in the PDII/TESPT-silica composite and decreased the viscosity of the compound which made the polymer chains more flexible and not easy to be crosslinked.

Thermal Properties of PDII Gum, Neat PDII, and PDII Composites

The typical DSC heating thermograms for PDII gum, neat PDII and PDII composites are shown in Figure 6. It can be seen that all the polymers were amorphous, with glass transition temperatures (T_g) ranging from −39.5 to −29.7°C, and no crystallization melting peaks are found. After crosslinking, the transition temperature increased from −39.5 to −31.7°C, which caused by the decreased of free volume after crosslinking. Additionally, with CB filled in, T_gs of the composites increased slightly from neat PDII. The explanation is that filler attached with the crosslinked PDII chains, thus, restricted the flexibility of the PDII polymer chains. However, T_gs of PDII/silica and PDII/TESPT-silica are lower than neat PDII. The decrease of T_g for

Applied Polymer SCIENCE

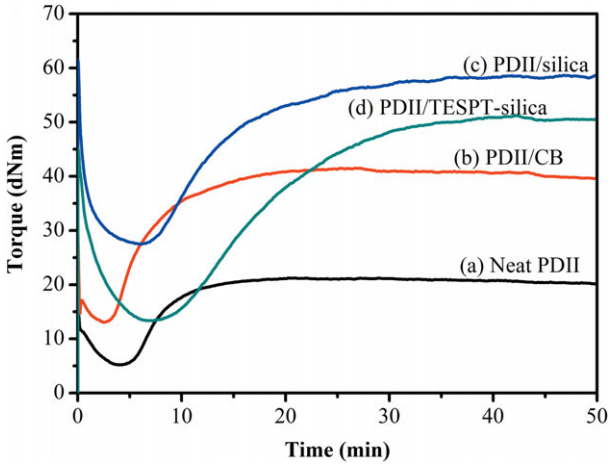

Figure 5. Cure curves of neat PDII and PDII composites. [Color figure can be viewed in the online issue, which is available at wileyonlinelibrary.com.]

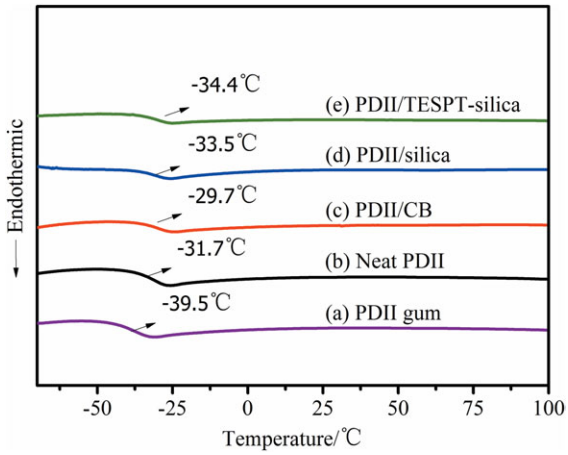

Figure 6. DSC thermograms of PDII gum and PDII composites. [Color figure can be viewed in the online issue, which is available at wileyonlinelibrary.com.]

silica-filled PDII may be caused by lower crosslink density than CB-filled PDII which caused by the adsorption of accelerator by silica.

Mechanical Properties of Neat PDII and PDII Composites

As shown in Table V, the tensile strength and stress at 100% strain of PDII composites are significantly higher than neat PDII. The elongation at break of PDII/CB remains about the same as that of neat PDII, but those of PDII/silica and PDII/TESPT-silica are significantly higher. Though the tensile strengths of PDII/silica and PDII/CB are basically the same, the stress at 100% strain of PDII/silica is less than PDII/CB. Furthermore, the elongation at break of PDII/silica and PDII/TESPT-silica is much higher than PDII/CB, indicating lower crosslink density owing to the adsorption of accelerators by silica. PDII reinforcement through nanoparticles led to the formation of stretched PDII macromolecular chains between neighboring particles induced by the slippage of macromolecular chains on the filler surface during stretching. The tensile strength increases from 9.15 MPa for PDII/silica to 11.22 MPa for PDII/TESPT-silica, but the elongation at break decreased from 440.8 to 410.7%.

Surface Tension of Neat PDII, SBR, NR, and Their Composites

Surface tension was evaluated using the surface tension-component theory.[41,42] According to this approach, surface tension of a solid phase (γ_S) could be divided into independent components such as London dispersion contribution γ_S^d and polar contribution γ_S^p. For a drop of liquid at equilibrium with a solid surface, the liquid–solid contact angle (θ) is given by:

$$\gamma_L(1+\cos\theta)/2(\gamma_L^d)^{1/2} = (\gamma_S^p)^{1/2}(\gamma_L^p\gamma_L^d)^{1/2} + (\gamma_S^d)^{1/2}$$

where γ_L is the surface tension of the liquid and subscripts S and L represent solid and liquid. Hence, by measuring contact angle for two well-characterized liquids, γ_S^d and γ_S^p could be obtained. In this study, water and glycol were used. For water, $\gamma_L = 72.8$ mJ/m^2, $\gamma_L^d = 51.0$ mJ/m^2, $\gamma_L^p = 21.8$ mJ/m^2 at 20°C. For glycol, $\gamma_L = 48.3$ mJ/m^2, $\gamma_L^d = 29.3$ mJ/m^2, $\gamma_L^p = 19.0$ mJ/m^2 at 20°C.

The variation of surface tension of PDII, SBR, NR, and their composites is summarized in Table VI. It is clear that surface tension of PDII, SBR, and NR increased after filling with silica. The polar contribution of PDII/silica is much higher than SBR/silica and NR/silica, indicating stronger interaction between PDII and silica than conventional rubbers. It should be contributed by the hydrogen bonding between PDII macromolecular chains and silica.

Table IV. Curing Parameters of Neat PDII and PDII Composites

Filler	Scorch time (min:s)	Optimum cure time (min:s)	Torque max (dNm)	Torque min (dNm)
Neat PDII	5:39	12:43	21.23	5.19
PDII/CB	3:50	14:14	41.51	13.03
PDII/silica	8:17	24:33	58.69	27.44
PDII/TESPT-silica	10:42	27:27	50.11	13.29

Dynamic Properties of Neat PDII and PDII Composites

The presence of these hard particles such as CB and silica in the soft polymer bulk significantly alters the dynamic and physical response of composites. Figure 7 shows the temperature dependence of tanδ of PDII and its various composites. The tanδ peak is obviously lower for the PDII composites than for neat PDII owing to the volume effect of fillers, indicating that the PDII composites were more elastic and had a smaller internal temperature rise under dynamic stress than neat PDII. Generally, the temperature associated with the peak magnitude of the tanδ plot is defined as T_g. Figure 7 shows that PDII/CB has a higher T_g than neat PDII, but the PDII/silica and PDII/TESPT-silica have lower T_g than neat PDII.

One of the main consequences of the addition of reinforcing fillers to an elastomer matrix is the alteration of dynamic properties as the presence of a filler network significantly affects the viscoelastic response of the material. This effect is observed in the temperature dependence of the elastic modulus component

Table V. Mechanical Properties of PDII and PDII Composites

Items	Tensile strength (MPa)	Stress at 100% strain (MPa)	Elongation at break (%)	Hardness shore A
Neat PDII	1.10 ± 0.10	0.29 ± 0.07	350.7 ± 10.5	60
PDII/CB	8.39 ± 0.22	1.89 ± 0.06	356.8 ± 9.3	70
PDII/silica	9.15 ± 0.22	1.53 ± 0.06	440.8 ± 9.3	78
PDII/TESPT-silica	11.22 ± 0.28	1.75 ± 0.12	410.7 ± 14.1	73

Table VI. Surface Tension of PDII, SBR, NR and Their Composites

Items	$\gamma_S^d/(10^{-3}$ N/m)	$\gamma_S^p/(10^{-3}$ N/m)	$\gamma_S/(10^{-3}$ N/m)
Neat PDII	21.2	7.6	28.8
Neat SBR	26.0	2.6	28.6
Neat NR	20.3	5.6	25.9
PDII/silica	17.4	18.6	36.0
SBR/silica	16.8	11.0	27.8
NR/silica	18.6	13.0	31.6

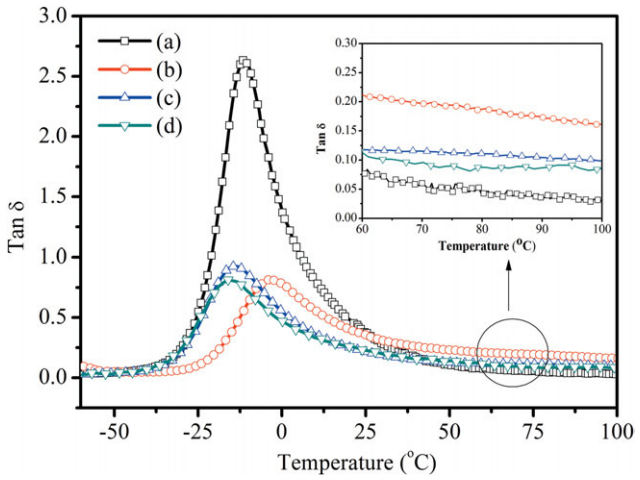

Figure 7. Tanδ of PDII and PDII composites versus temperature by DMTA (a) neat PDII, (b) PDII/CB, (c) PDII/silica, and (d) PDII/TESTP-silica. [Color figure can be viewed in the online issue, which is available at wileyonlinelibrary.com.]

(E'). The storage modulus is a measure of the elasticity of rubbery material under periodic deformation in DMTA. As shown in Figure 8, the neat PDII shows a lower elastic modulus across the whole temperature range than the PDII composites. Between −35 and 30°C, PDII/CB shows a higher storage modulus than those of PDII/silica and PDII/TESPT-silica, indicating stronger interaction of PDII with CB than silica. In the glassy state (below −35°C) and viscous state (above 50°C), the PDII composites show about the same storage modulus.

CONCLUSIONS

CB and silica were used to reinforce a novel PDII elastomer. Homogeneous dispersion of silica and CB in the PDII matrix was confirmed by SEM and TEM. Hydrogen bonds between

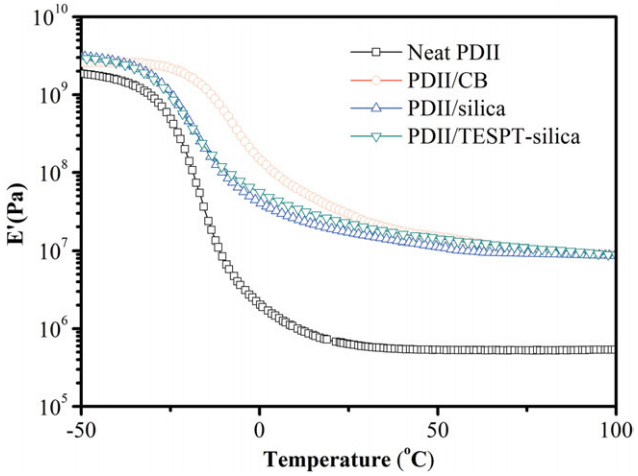

Figure 8. Storage modulus of PDII and PDII composites versus temperature. [Color figure can be viewed in the online issue, which is available at wileyonlinelibrary.com.]

silica and PDII macromolecules were characterized and confirmed by FTIR. The hydrogen bonds restrained the agglomeration of silica particles which contributed to the homogeneous dispersion of silica in the PDII matrix. The adsorption of the accelerators by silica made cure rate and crosslink density of PDII/silica and PDII/TESPT-silica lower than PDII/CB. Furthermore, the tensile strength of PDII/silica was comparable with PDII/CB, but PDII/TESPT-silica had higher tensile strength. As silica is independent of petroleum, PDII reinforced by silica or modified silica could be a good candidate for replacing rubbers based on the petroleum resources.

ACKNOWLEDGMENTS

This study was supported by National Natural Science Foundation of China (50933001), National Outstanding Youth Science Fund (50725310), and National Basic Research Program (973 Program) of China (2011CB606003). Thanks for the financial support of Goodyear Tire & Rubber Company.

REFERENCES

1. Liu, Q.; Jiang, L.; Shi, R.; Zhang, L. *Prog. Polym. Sci.* **2012**, *37*, 715.
2. Amsden, B. *Soft Matter.* **2007**, *3*, 1335.
3. Muller, G.; Rieger, B. *Prog. Polym. Sci.* **2002**, *27*, 815.
4. Gandini, A. *Macromolecules* **2008**, *41*, 9491.

5. Barrett, D. G.; Merkel, T. J.; Luft, J. C.; Yousaf, M. N. *Macromolecules* **2010**, *43*, 9660.
6. Yang, J.; Webb, A. R.; Ameer, G. A. *Adv. Mater.* **2004**, *16*, 511.
7. Lee, K. Y.; Mooney, D. J. *Chem. Rev.* **2001**, *101*, 1869.
8. Buttafoco, L.; Kolkman, N. G.; Engbers-Buijtenhuijs, P.; Poot, A. A.; Dijkstra, P. J.; Vermes, I.; Feijen, J. *Biomaterials* **2006**, *27*, 724.
9. Chen, R.; Curran, S. J.; Curran, J. M.; Hunt, J. A. *Biomaterials* **2006**, *27*, 4453.
10. Martina, M.; Hutmacher, D. W. *Polym. Int.* **2007**, *56*, 145.
11. Bruggeman, J. P.; de Bruin, B.-J.; Bettinger, C. J.; Langer, R. *Biomaterials* **2008**, *29*, 4726.
12. Langer, R.; Peppas, N. A. *AlChE J.* **2003**, *49*, 2990.
13. Langer, R. S.; Peppas, N. A. *Biomaterials* **1981**, *2*, 201.
14. Yang, J.; Webb, A. R.; Pickerill, S. J.; Hageman, G.; Ameer, G. A. *Biomaterials* **2006**, *27*, 1889.
15. Mitsuyasu, O.; Dwiarti, L.; Shin, K. *Appl. Biochem. Biotechnol.* **2009**, *84*, 597.
16. Fortman, J. L.; Chhabra, S.; Mukhopadhyay, A.; Chou, H.; Lee, T. S.; Steen, E.; Keasling, J. D. *Trends Biotechnol.* **2008**, *26*, 375.
17. Piang-Siong, W.; de Caro, P.; Lacaze-Dufaure, C.; Sing, A. S. C.; Hoareau, W. *Ind. Corp. Prod.* **2012**, *35*, 203.
18. Bandres, M.; de Caro, P.; Thiebaud-Roux, S.; Borredon, M.-E. *C. R. Chim.* **2011**, *14*, 636.
19. Singh, R. *Org. Process Res. Dev.* **2010**, *15*, 175.
20. Yang, J.; Zhao, G.; Sun, Y.; Zheng, Y.; Jiang, X.; Liu, W.; Xian, M. *Biores. Technol.* **2012**, *104*, 642.
21. Hamed, G. R. *Rubber Chem. Technol.* **2000**, *73*, 524.
22. Edwards, D. C. *J. Mater. Sci.* **1990**, *25*, 4175.
23. Karásek, L.; Sumita, M. *J. Mater. Sci.* **1996**, *31*, 281.
24. Wolff, S. *Rubber Chem. Technol.* **1996**, *69*, 325.
25. Park, S.-J.; Cho, K.-S. *J. Colloid Interface Sci.* **2003**, *267*, 86.
26. Rueda, L. I.; Antón, C. C.; Rodriguez, M. C. T. *Polym. Compos.* **1988**, *9*, 198.
27. Gopalan Nair, K.; Dufresne, A. *Biomacromolecules* **2003**, *4*, 657.
28. Yue, D.; Liu, Y.; Shen, Z.; Zhang, L. *J. Mater. Sci.* **2006**, *41*, 2541.
29. Varghese, S.; Karger-Kocsis, J. *Polymer* **2003**, *44*, 4921.
30. Suzuki, N.; Ito, M.; Yatsuyanagi, F. *Polymer* **2005**, *46*, 193.
31. Sun, C. C.; Mark, J. E. *Polymer* **1989**, *30*, 104.
32. Choi, S.-S.; Nah, C.; Lee, S. G.; Joo, C. W. *Polym. Int.* **2003**, *52*, 23.
33. Hashim, A. S.; Azahari, B.; Ikeda, Y.; Kohjiya, S. *Rubber Chem. Technol.* **1998**, *71*, 289.
34. Choi, S. S. *Polym. Adv. Technol.* **2002**, *13*, 466.
35. Choi, S. S.; Park, B. H.; Song, H. *Polym. Adv. Technol.* **2004**, *15*, 122.
36. Vo, L. T.; Anastasiadis, S. H.; Giannelis, E. P. *Macromolecules* **2011**, *44*, 6162.
37. Mora-Barrantes, I.; Ibarra, L.; Rodriguez, A.; Gonzalez, L.; Valentin, J. L. *J. Mater. Chem.* **2011**, *21*, 17526.
38. Cowie, J. M. G.; Henshall, S. A. E.; McEwen, J. *Polymer* **1977**, *18*, 612.
39. Cheong, I. W.; Fellows, C. M.; Gilbert, R. G. *Polymer* **2004**, *45*, 769.
40. Stoffelbach, F. O.; Tibiletti, L.; Rieger, J.; Charleux, B. *Macromolecules* **2008**, *41*, 7850.
41. Zhang, J.; Xue, Z. *Polym. Test.* **2011**, *30*, 753.
42. Owens, D. K.; Wendt, R. C.; *J. Appl. Polym. Sci.* **1969**, *13*, 1741.